

Modeling of the parametric dependence of the edge toroidal rotation for MAST and ASDEX Upgrade

V. Rozhansky^{a,*}, P. Molchanov^a, S. Voskoboynikov^a, G. Counsell^b,
A. Kirk^b, D. Coster^c, R. Schneider^d

^a St. Petersburg State Polytechnical University, Polytechnicheskaya 29, 195251 St. Petersburg, Russia

^b EURATOM/UKAEA Fusion Association, Culham Science Centre, Abingdon, Oxon OX14 3DB, UK

^c Max-Planck Institut für Plasmaphysik, EURATOM-Association, Garching, Germany

^d Max-Planck Institut für Plasmaphysik, EURATOM-Association, Greifswald, Germany

Abstract

Modeling of the edge toroidal rotation and its dependence on the edge plasma parameters is performed by means of the B2SOPS5.0 transport code for Ohmic shots both for MAST and ASDEX Upgrade configurations. The impact of plasma current, toroidal magnetic field, plasma density and temperature is investigated. A connection between the toroidal rotation and edge radial electric field is also studied. The results of the simulation are consistent with the parametric dependence predicted analytically.

© 2007 Published by Elsevier B.V.

PACS: 52.25.Fi; 52.55.Fa; 52.65.-y

Keywords: Edge modeling; MAST; ASDEX Upgrade

1. Introduction

Spontaneous generation of toroidal rotation in the core of a tokamak is one of the most interesting findings of recent years. There are some experimental indications, e.g. dependence of the central toroidal rotation on the divertor configuration [1], that the edge toroidal rotation is the key parameter, which might determine the core rotation. Hence the study of the edge toroidal rotation and its parametric dependence is currently one of the

main tasks. In the present paper modeling of the edge toroidal rotation and its dependence on edge plasma parameters is performed by means of the B2SOPS5.0 transport code for Ohmic shots for both MAST and ASDEX Upgrade (AUG). The impact of plasma current, toroidal magnetic field, plasma density and temperature is investigated. A connection between the toroidal rotation and edge radial electric field is also studied.

2. Simulation results

Two Ohmic shots were chosen for simulation: no. 13009 for MAST and no. 19415 for AUG. For

* Corresponding author. Fax: +7 812 5527954.

E-mail address: rozhansky@phtf.stu.neva.ru (V. Rozhansky).

MAST the following transport coefficients were taken: perpendicular diffusion coefficient $D = 3 \text{ m}^2/\text{s}$, electron and ion thermal diffusivities $\kappa_e/n_e = 5 \text{ m}^2/\text{s}$, $\kappa_i/n_e = 5 \text{ m}^2/\text{s}$. Plasma parameters on the inner boundary of the simulation domain were: $n_e|_{\text{core}} = 1.75 \times 10^{19} \text{ m}^{-3}$, $T_e|_{\text{core}} = T_i|_{\text{core}} = 192 \text{ eV}$. For the AUG case the parameters used were: $D = 0.28 \text{ m}^2/\text{s}$, thermal diffusivities $\kappa_e/n_e = 0.435 \text{ m}^2/\text{s}$, $\kappa_i/n_e = 0.516 \text{ m}^2/\text{s}$, $n_e|_{\text{core}} = 2.85 \times 10^{19} \text{ m}^{-3}$, $T_e|_{\text{core}} = T_i|_{\text{core}} = 400 \text{ eV}$. Simulations were then performed

in which the density, electron and ion temperature, plasma current and toroidal magnetic field were changed independently to investigate the parametric dependence of the toroidal rotation and the radial electric field. Other parameters were kept constant. The results for the toroidal rotations are shown in Figs. 1 and 2. In these figures plotted is parallel velocity directly obtained from the code, which is rather close to the toroidal velocity. To check the role of drifts simulations were performed in which they were switched on and off. One can see that for both MAST and AUG the toroidal rotation at the outer mid-plane is mainly caused by the drifts

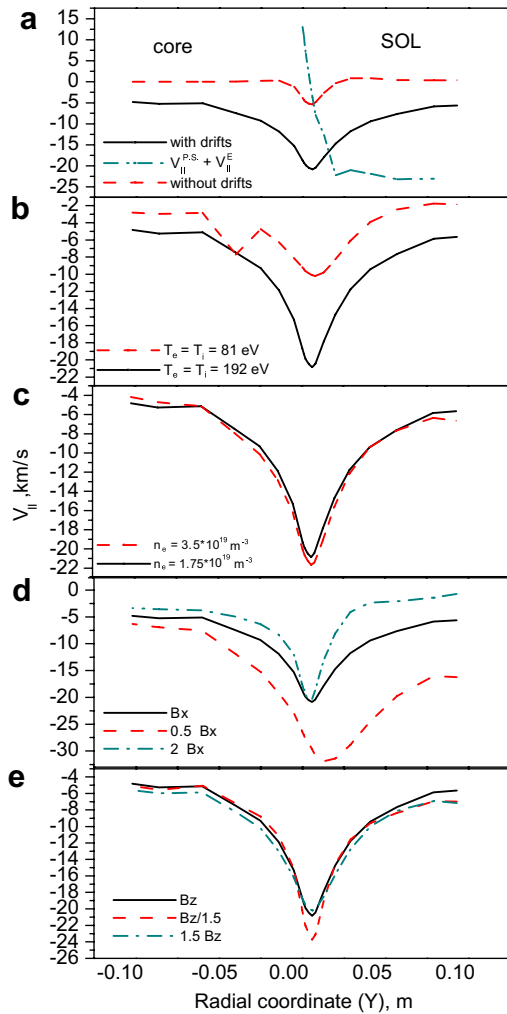


Fig. 1. Toroidal rotation velocity in MAST, shot No 13009: (a) with and without drifts and sum of Pfirsch–Schlueter velocity and the velocity compensating the $\vec{E} \times \vec{B}$ drift; (b) different temperatures $T_e = 192 \text{ eV}$ and $T_e = 81 \text{ eV}$; (c) different densities $n_e = 3.5 \cdot 10^{19} \text{ m}^{-3}$ and $n_e = 1.7 \cdot 10^{19} \text{ m}^{-3}$, (d) different poloidal magnetic fields $B_x = 0.42 \text{ T}$, $B_x = 0.21 \text{ T}$, $B_x = 0.84 \text{ T}$; (e) different toroidal magnetic fields $B_z = 1.9 \text{ T}$, $B_z = 1.3 \text{ T}$, $B_z = 2.9 \text{ T}$.

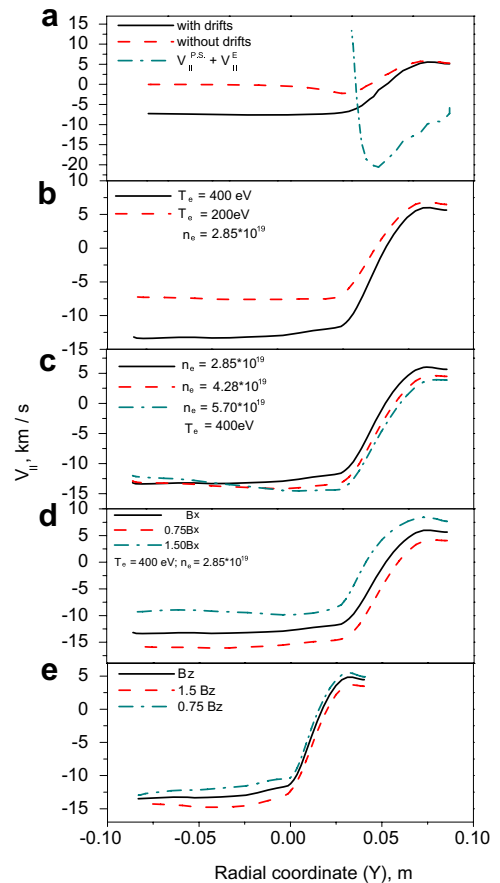


Fig. 2. Toroidal rotation velocity in ASDEX Upgrade, shot no. 18737. (a) with and without drifts and sum of Pfirsch–Schlueter velocity and the velocity compensating the $\vec{E} \times \vec{B}$ drift; (b) different temperatures $T_e = 400 \text{ eV}$ and $T_e = 200 \text{ eV}$; (c) different densities $n_e = 2.85 \cdot 10^{19} \text{ m}^{-3}$, $n_e = 4.28 \cdot 10^{19} \text{ m}^{-3}$, and $n_e = 5.7 \cdot 10^{19} \text{ m}^{-3}$ (d) different poloidal magnetic fields $B_x = 0.29 \text{ T}$, $B_x = 0.22 \text{ T}$, $B_x = 0.44 \text{ T}$; (e) different toroidal magnetic fields $B_z = 1.6 \text{ T}$, $B_z = 2.4 \text{ T}$, $B_z = 1.2 \text{ T}$.

(the negative sign corresponds to the co-current direction). The toroidal rotation has a weak dependence on density and toroidal magnetic field. The absolute value of the toroidal rotation velocity is smaller for lower temperatures and is larger for smaller poloidal magnetic field.

The radial electric field, Figs. 3 and 4, depends mainly on temperature; it is roughly proportional to the separatrix temperature. The dependence of the radial electric field on density and toroidal magnetic field is rather weak. There is almost no dependence on the poloidal magnetic field for AUG and some dependence is observed for MAST.

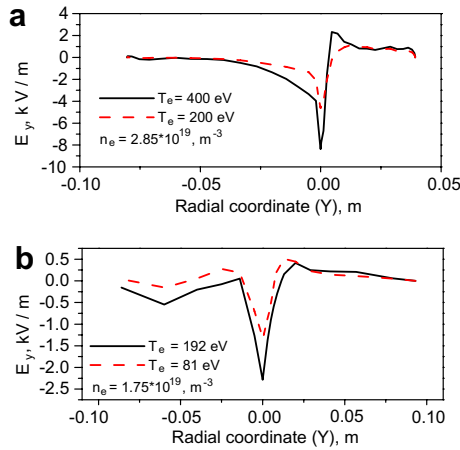


Fig. 3. Radial electric field for AUG (a) and MAST (b). Temperature scan.

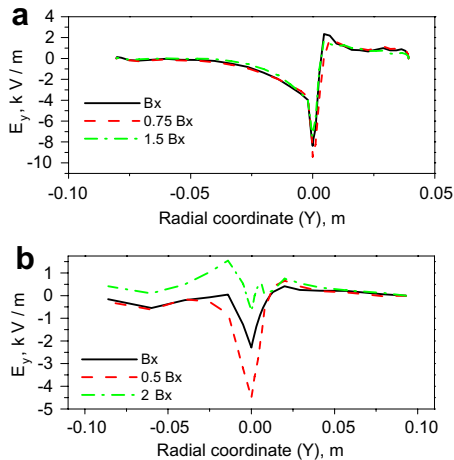


Fig. 4. Radial electric field for AUG (a) and MAST (b). Poloidal magnetic field scan.

3. Discussion

The toroidal rotation in the scrape-off layer (SOL) of a tokamak is a complicated phenomenon. However, it is possible to trace three contributions to the parallel flows, which are rather close to the toroidal ones, Fig. 5. The first one is the Pfirsch–Schlueter (PS) flow, which arises to close the vertical ∇B drift of ions. The expression for the PS velocity, with the assumption of poloidally independent pressure (for more sophisticated expression see [2]), is

$$V_{\parallel}^{\text{PS}} = \left(\frac{1}{en h_y} \frac{\partial p_i}{\partial y} + \frac{1}{h_y} \frac{\partial \phi}{\partial y} \right) \frac{B_z}{B_x B} \left(1 - \frac{B^2}{\langle B^2 \rangle} \right), \quad (1)$$

where x is the poloidal co-ordinate, y is the radial co-ordinate, z is the toroidal co-ordinate, $h_x = \frac{1}{\|\nabla_x\|}$, $h_y = \frac{1}{\|\nabla_y\|}$, $h_z = \frac{1}{\|\nabla_z\|}$ are metric coefficients, $h_x h_y h_z = \sqrt{g}$.

Since the radial electric field in the SOL is positive and the ion pressure is decreasing with radius, the PS flow is maximal in absolute value at the outer and inner equatorial mid-planes and is zero at the top and bottom. It is an upper estimate of the flow. The poloidal dependence of the ion pressure is accounted for by the addition of another term in the *right hand side* of particle balance equation, which is absent in the core: $\frac{1}{\sqrt{g}} \frac{\partial}{\partial y} \left[\left(\frac{1}{\langle B^2 \rangle} - \frac{1}{B^2} \right) \frac{h_x B_z}{e} \frac{\partial n T_i}{\partial x} \right]$. It can be shown that this term leads to a decrease of the absolute value of V_{\parallel} with respect to $V_{\parallel}^{\text{PS}}$.

The second flow is the flow compensating the $\vec{E} \times \vec{B}$ drift in the radial electric field to keep the

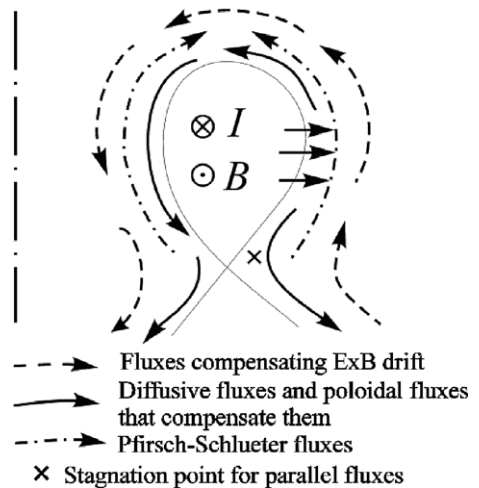


Fig. 5. Scheme of the parallel fluxes in the SOL.

same poloidal flow in the presence of drifts as without drifts. The corresponding value is

$$V_{\parallel}^E = \frac{1}{B_x} \frac{\partial \phi}{h_y \partial y}. \quad (2)$$

Finally there is also parallel unbalanced flow, which is not connected with drifts and is directed towards the plates in the divertor regions. In the SOL this flow is often directed from the outer to the inner plates due to the larger radial flow through the outer part of the torus and temperature asymmetries at the plates (hotter outer plates). This pattern is supported by the results of simulations when the drifts were switched off. Due to viscosity coupling, these parallel fluxes are transported through the separatrix and thus a similar parallel flow pattern is created in the core as in the separatrix vicinity (inside the viscous layer).

It is difficult to predict the parametric dependence of the unbalanced parallel flow (not connected with drifts). In contrast, the other part of the parallel flow, which is given by Eqs. (1) and (2), might be analyzed. First, since both pressure and potential in the SOL are proportional to the temperatures, one would expect larger contribution to the toroidal rotation for larger temperatures. This is consistent with the simulation results both for MAST and AUG. The inverse dependence of the toroidal rotation value on the poloidal magnetic field observed in the simulations is again consistent with Eqs. (1) and (2). Finally, since part of the parallel flow Eqs. (1) and (2) is density independent one might expect the absence of a density dependence, which is indeed observed in the simulations. The same weak dependence on the toroidal magnetic field is again consistent with the simulation results (for MAST this might be a bit more complicated since the toroidal magnetic field B_z and full magnetic field B are different).

Note that the parametric scan in the simulations was performed with other parameters being constant. In real Ohmic shots, however, the density rise would cause a simultaneous temperature drop, the current rise could cause a temperature rise, etc. Hence modeling of real Ohmic shots and comparison with Mach probe measurements should be performed. In AUG measurements of the toroidal velocity profile in the SOL were performed for two Ohmic shots with different densities [3]. The toroidal Mach number profiles for the two shots were similar and the shape of the radial profile matched those obtained in the simulations, Fig. 6, see also

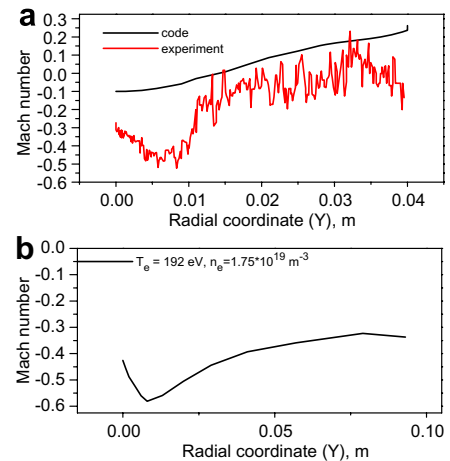


Fig. 6. Mach number for AUG shot no. 18737 (a) and MAST shot no. 13009 (b).

[4]. However, the absolute value in the experiment was larger – about $M = 0.5$ near the separatrix.

The dependence of radial electric field on the local parameters has been analyzed earlier; see [5] and references therein. The results presented are consistent with neoclassical character of the radial electric field.

4. Conclusions

1. In Ohmic discharges the toroidal rotation at the low field side equatorial mid-plane is co-current directed.
2. The density and toroidal magnetic field dependence is rather weak.
3. The absolute value of the toroidal rotation is larger for larger edge temperatures.
4. The absolute value of the toroidal rotation is larger for smaller plasma currents (poloidal magnetic fields).
5. The parametric dependence of the toroidal rotation is similar to the parametric dependence of the Pfirsch–Schlueter parallel flows and parallel flows compensating $\vec{E} \times \vec{B}$ drifts.

Acknowledgements

The work was supported by grants RFFI 06-02-16494, 06-02-08014-ofi. This work was funded jointly by the United Kingdom Engineering and Physical Sciences Research Council and by the European Communities under the contract of Association between EURATOM and UKAEA. The

views and opinions expressed herein do not necessarily reflect those of the European Commission.

References

- [1] J.E. Rice et al., Nucl. Fusion 45 (2005) 251.
- [2] V. Rozhansky et al., Nucl. Fusion 43 (2003) 614.
- [3] H.W. Muller et al., Proceedings 32 EPS Conference Plasma Phys. Control. Fus. P-1.009.
- [4] D. Coster et al., Proceedings 32 EPS Conference Plasma Phys. Control. Fus. P-1.008.
- [5] V. Rozhansky, Plasma Phys. Control. Fus. 46 (2004) A1.